International Journal of Academic Multidisciplinary Research (IJAMR)
ISSN: 2000-006X
Vol. 2 Issue 11, November – 2018, Pages: 1-6

Magnetoelectric Properties of $La_{0.7}Sr_{0.3}Fe_{1-x}Ni_xO_3$; $0.0 \leq x \leq 0.2$ Multiferroics System

Prof. Dr. Ragab R. Amin[a], Ahmed A. Gomma[b].

a. Basic Science Department, Nahda University, Faculty of Engineering, Beni Suef, Egypt.
b. Basic Science Department, Nahda University, Faculty of Engineering, Beni Suef, Egypt.

Corresponding author:
Prof. Dr. Ragab R. Amin;
E. mail. **Ragab.amin@nub.edu.eg. ,**
Fax: +2 082 2284688

Abstract: *In this study, the bulk ceramics with general formula La0.7Sr0.3Fe1-xNixO3; 0.0 ≤ x ≤ 0.2 nanocrystalline samples were successfully prepared by citrate autocombustion technique. The effect of Ni2+ ion substitution on the AC electrical conductivity and dielectric properties at different frequencies 400 KHz to 5MHz was studied. The obtained data reveal that ε/, and tanδ increase as Ni2+ ion increases due to the increase the number of vacancies at the B site as Ni2+ content increases. The magneto-electric coefficient was measured for all nanomultiferroics samples and ferroelectric properties was examined for all prepared samples as well as and the data obtained that the higher value of magneto-electric coefficient at x=0.2.*

Keywords: AC conductivity; Dielectric constant; Multiferroics; Nanoparticle.

1. INTRODUCTION

In certain insulating materials possessing magnetism and ferroelectricity simultaneously, spontaneous magnetization can be switched by an electric field and vice versa, spontaneous polarization can be switched by a magnetic field. This phenomenon is known as magnetoelectric effect. Such effect has been observed in two-phase ferrite-ferroelectric composites [1, 2]. Also this effect has been observed in certain single-phase materials such as Cr_2O_3, Gd_2CuO_4, $EmMn_2O_4$, etc. [3–5].

Spin related exchange interaction, also referred to as superexchange, is the antiferromagnetic coupling between two next-to-nearest neighbor positive ions through a non-magnetic anion, such as oxygen [6]. It strongly depends on the electronic and crystallographic structure such as electron occupancy, orbital configuration and geometry, respectively [7]. In the case of double exchange, the electrons move between positive ions having different d-shell occupancy via a non-magnetic anion [8]. The electronic conductivity of perovskites is generally explained in terms of small polarons which are thermally activated [9]. The electrons hop from one side to the other via B–O–B bridge which are mostly increased by overlap (strongly depends on the B–O distance and B–O–B superexchange angle [10]. A-site substitution in iron perovskites is well studied and relatively well understood. B site substitution is less well studied.

The electronic conductivity of perovskites is generally explained in terms of small polarons which are thermally activated [9]. The electrons hop from one side to the other via B–O–B bridge which are mostly increased by overlap (strongly depends on the B–O distance and B–O–B superexchange angle [10]. A-site substitution in iron perovskites is well studied and relatively well understood. B site substitution is less well studied. At the molecular scale, the structure of the perovskite includes the valence state of the A-site and B-site cations, and the spin state of the B-site cations, and the oxygen deficiency. $LaFeO_3$ is a well known ABO_3 perovskite with orthorhombic symmetry (a=5.5647Å, b=7.8551Å, and c=5.5560Å) and an antiferromagnetic insulator with a Neel temperature T_N=750K [11]. When the trivalent La is substituted by the divalent Sr, which also has a larger ion radius than La, one electron hole is created at the oxygen site, and the size difference constitutes a chemical pressure [12]. This effect decreases the rhombohedral lattice distortion.

In the present work we discuss the changes in the crystallographic structure upon Ni^{2+}doping (i. e. symmetry, Fe/Ni–O distance, superexchange angle) which affect hopping process (Fe^{3+}–O^{2-}– Fe^{3+}/Fe^{4+}) with either superexchange or double exchange and charge transfer process and consequently electronic conductivity. An increase in Tolerance factor is paralleled to an increase in symmetry. We also discuss the effect of the B-site Coulomb potential which plays an important role on the conductivity.

2. EXPERIMENTAL PROCEDURE

$La_{0.7}Sr_{0.3}Fe_{1-x}Ni_xO_3$; $0.0 \leq x \leq 0.2$ nanocrystalline samples were successfully prepared by the citrate-nitrate auto-combustion method [13]. The molar ratio of metal nitrates to citric acid was 1: 1. A small amount of ammonia was added to the solution to adjust the pH value at 7. The precursor mixture was then heated to allow evaporation and to obtain a dried product in the form of uniformly colored gray fibers containing all the cations homogenously mixed together at the atomic level. After cooling to room temperature it was

grinded properly for half an hour in an agate mortar. The details of the preparation method were illustrated in the flowchart.

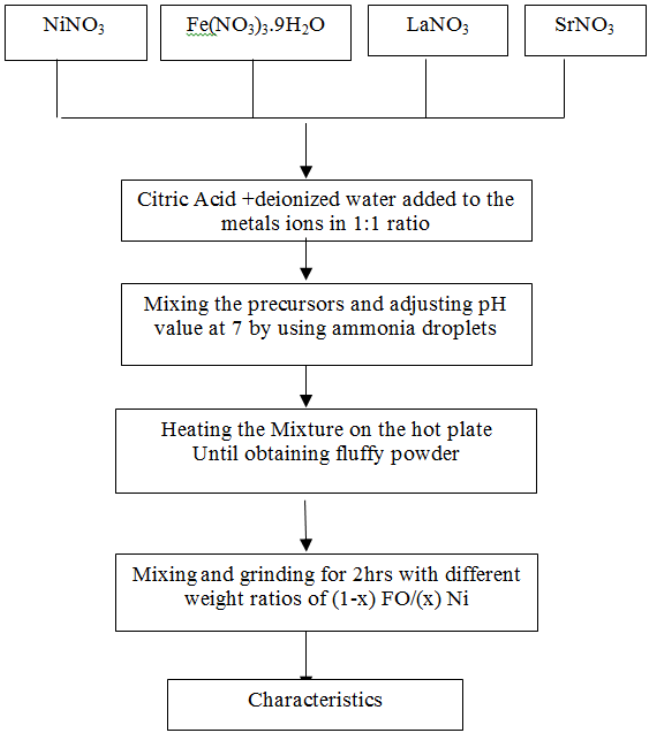

The two surfaces of the sample were good polished to obtain uniform thickness and coated by silver paste and checked for good conduction to be ready for measuring the dielectric properties and the ac conductivity (σ_{ac}) using Hioki LCR Hitester type 3531 (Japan) as a function of temperature from 300 to 800K and frequencies from 100kHz to 5MHz. The temperature was measured using T-type thermo-couple with junction in contact with the sample.

The accuracy of measuring temperature was better than ±1°C. The thermoelectric power (α) was calculated using the relation: $\alpha = \Delta V/\Delta T$; where ΔV is the potential difference measured across the surfaces of the sample, ΔT is the temperature difference between the two surfaces of the sample which is fixed at ≈10°C.

3. RESULTS AND DISCUSSION:

3. 1. IR Absorption Studies:

The vibrational spectrum of a molecule is considered to be a unique physical property and is a characteristic of the molecule. As such infrared spectrum can be used as a fingerprint by the comparison of the spectrum from 'unknown' spectrum. Fig. (1) Shows the infrared spectrum of the $La_{0.7}Sr_{0.3}Fe_{1-x}Ni_xO_3$; x= 0.0, 0.05, 0.1, 0.15 and 0.2 nanomultiferroics samples. The absorption band around 585cm^{-1} is attributed to Fe–O stretching normal vibrations, while the absorption band at 350 cm^{-1} is attributed to Fe–O bending vibrations. All other samples show prominently two absorption peaks. Similar IR absorption spectra were obtained in the case of other rare earth orthoferrites [14]. The infrared absorption data is presented in Table 1. It has been observed that the broadness of absorption peaks is greater at smaller concentration of Ni in $La_{0.7}Sr_{0.3}Fe_{1-x}Ni_xO_3$; x= 0.0, 0.05, 0.1, 0.15 and 0.2. Two absorption peaks become much broader and. This change may be due to a change in the distortion of the structure as observed in tolerance factor calculations.

Ni content (x)	v1(cm^{-1})	v2 (cm^{-1})	v3 (cm^{-1})	v4 (cm^{-1})
0	583	345	1457	3436
0.05	587	351	1458	3440
0.1	585	345	1456	3436
0.15	586	354	1456	3432
0.2	587	361	1457	3429

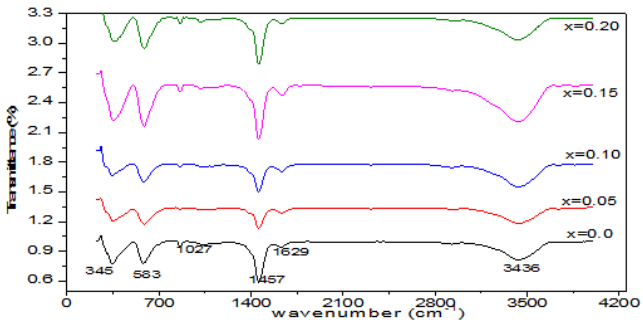

Fig.(1) IR spectrum of $La_{0.7}Sr_{0.3}Fe_{1-x}Ni_xO_3$; x= 0.0, 0.05, 0.1, 0.15 and 0.2 nanomultiferroics.

3.2. Electrical Properties:

3.2.1. Temperature dependence of dielectric constant and dielectric loss at different frequencies:

The variation of dielectric constant of ferrite has been mainly attributed to the variation in concentration of Fe^{2+} and its valence. The greater the concentration of these ions, the higher the dielectric constant is expected. The presence of Fe^{2+} ions results in charge transfer of the type $Fe^{2+} \leftrightarrow Fe^{3+} + e^-$, causing a local displacement of electron in the direction of electric field leading to polarization[15]. The dielectric loss (tanδ) in ferrite is a measure of lag in the polarization with respect to the alternating field. The behavior of (tanδ) in ferrites is normally reflected in the resistivity measurements, with higher resistivity materials exhibiting low dielectric losses and vice versa. In most solids, the dielectric constant dependence on the variation of external factors such as temperature and frequency. The electron exchange interaction results in a local displacement of the electrons in the direction of the field which determine the polarization direction [15].

Figure (2) shows the variation of dielectric constant ε' for $La_{0.7}Sr_{0.3}Fe_{1-x}Ni_xO_3$; x= 0.0, 0.05, 0.1, 0.15, and 0.2 nanomultiferroics samples as a function of temperature and at frequencies (400 kHz-5MHz). The dielectric constant increases with temperature, which is the normal behavior in

most of the ferrites [16, 17]. Since, the charge hopping is thermally activated process, dielectric polarization increases with increasing temperature but with different rates resulting into an increase in the dielectric constant. In the first temperature region (T≤500K) a slow increase in $\varepsilon^{/}$ was obtained or nearly constant, because the thermal energy given to the sample was not sufficient enough to free the localized dipoles to be oriented in the field direction. At high frequencies, the friction between the dipoles increases leading to an increase in the quantity of heat generated and dissipated inside the sample thus the aligned dipoles will be disturbed with the result of decreasing $\varepsilon^{/}$. At T>500K, the thermal energy is quite sufficient to liberate more localized dipoles and the field aligned them in its direction, according $\varepsilon^{/}$ increases.

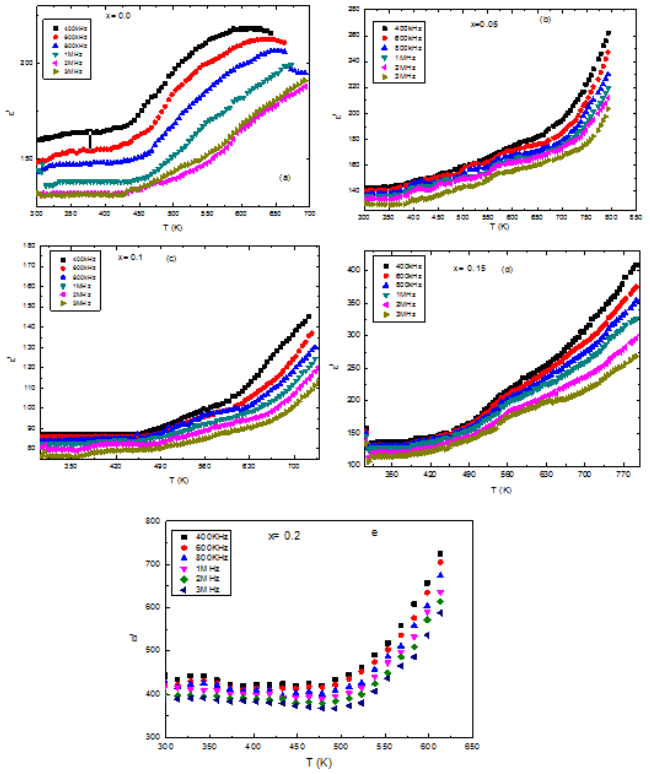

Fig.(2:a-e) Temperatures dependence of dielectric constant(ε/) for $La_{0.7}Sr_{0.3}Fe_{1-x}Ni_xO_3$; x= 0.0, 0.05, 0.1, 0.15, and 0.2 nanocrystalline samples at different frequencies.

The temperature dependence of the dielectric loss factor ($\varepsilon^{//}$) at different frequencies is illustrated in Fig. (3:a-e) for all LSNFO nanosamples under investigation. Generally, the dielectric loss factor increases with temperature due to the increase in the conductivity as

$$\sigma = \varepsilon^{/} \tan\delta \, 2\pi f \qquad (3.1)$$

The increase in thermal energy offers more degree of freedom for the charge carriers to hop between different localized states and the friction between dipoles increases the thermal agitation there by decreases the internal viscosity. At high frequencies, conductivity is revealed since the charge carriers have no time to detected or to feel the blocking boundaries (insulating phase) up to a certain limit where the electron – phonon scattering decreases the mobility of charge carriers.

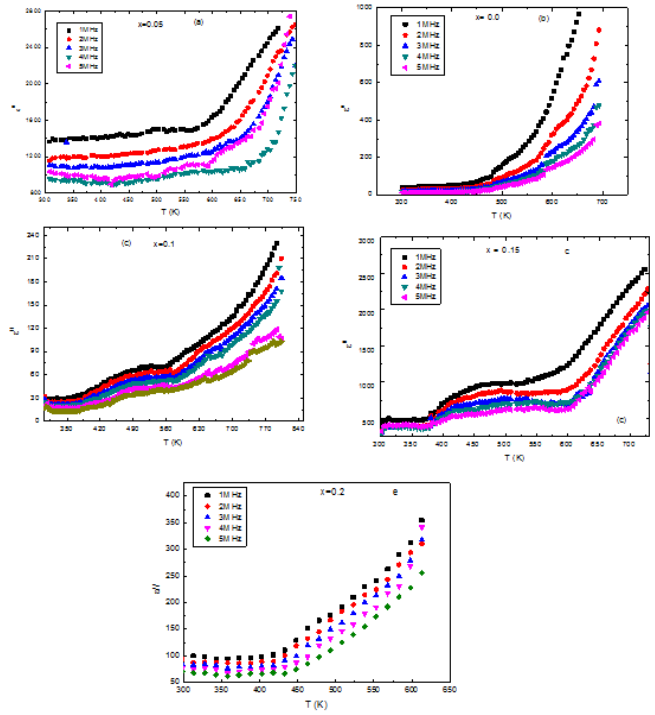

Fig.(3:a-e) Temperatures dependence of dielectric constant($\varepsilon^{//}$) for $La_{0.7}Sr_{0.3}Fe_{1-x}Ni_xO_3$; x= 0.0, 0.05, 0.1, 0.15, and 0.2 nanocrystalline samples at different frequencies.

3.2.2. Electrical conductivity:

The electrical conductivity is caused by the conducting electron hole hopping process from Fe^{3+} to Fe^{4+} via oxygen Bridge (Fe^{3+}–O^{2-}–Fe^{4+}) in LSNFO, and we concluded that charge transfer from oxygen to nickel (O–Ni) contributes additionally to electrical conductivity in LSFN [18]. Oxygen vacancies which interrupt the bridges between O and Fe/Ni are undesirable not only from the point of hopping but also from the point of charge transfer contributions.

The sample with x=0 having antiferromagnetic Fe^{3+}–O^{2-}–Fe^{3+} [19] and spin related superexchange interaction shows the least charge transfer. The charge transfer mainly depends on the overlap between O 2p and Ni 3d orbitals and is maximum when the <Ni–O–Ni> superexchangeangleis180° (cubic symmetry) or, in other words <ω>=0. Since this sample is in orthorhombic symmetry it has the largest deviation from the ideal cubic symmetry <Ni–O–Ni> superexchange angle (tilting angle) is around160° with

highest M–O distance due to strong A-site Coulomb potential and least charge transfer consequently. The sample with x=0.2 has ferromagnetic Fe^{3+}–O^{2-}–Fe^{4+} [19] hopping process with double exchange interaction where the conducting electrons jump from Fe^{3+} toward Fe^{4+} via the O bridge. The B-site potential decreases when Fe^{3+} is replaced by Ni^{2+}, resulting in a decrease in O–Fe/Ni distance, an increase in the O 2p bandwidth, and consequently an increase in mobility of the double exchange electrons and an increase in concentration of charge transferred electrons to Ni. Since the symmetry changes which leads to the distortion is reduced (<ω>=8.62°) resulting in an increase in <Fe/Ni–O–Fe/Ni> superexchange angle of around 163°.

3.2.1. Frequency dependence of electric conductivity at different temperature:

Figure (4: a,b) represents the variation of lnσ vs. ln(ω), 2πf for x=0.05 and 0.2 nanosamples as examples, at different temperatures. The data reveal more than one straight lines. The common feature of semiconductors is that, frequency dependent. Conductivity increases linearly [20]. In the present studied materials, the total conductivity at a given frequency is considered as $\sigma_{total}(\omega) = \sigma_o + \sigma(\omega)$ where σ_o is the dc conductivity due to band conduction and σ(ω) is the ac conductivity due to hopping conduction. The conductivity σ(ω) obeys the empirical formula of frequency dependence given by the ac power law:

$\sigma(\omega) = B(T)\,\omega^{s(T)}$ where B(T) is constant and the exponent s (T) ≤ 1. The ac power law regime of the conductivity at high frequency has been widely observed in systems involving correlated hopping transport as for ionic. The fractional exponent s is a measure of the degree of correlation between σ(ω) and frequency where, s should be zero for random hopping (i.e. σ_o is frequency independent) and tends to one as correlation increases (i.e. σ is frequency dependent).

In general, the dependence of s on temperature is a function of the conduction mechanism. Qualitatively, small polarons (SP) are usually associated with increase in s with an increasing temperature, while correlated barrier hopping (CBH) shows a decrease in s with increasing temperature. The results of ln(σ) versus ln(ω) graph when fitted to the equation;

lnσ=lnB(T)+sln(ω) yields values of both s and lnB(T). (3.2)

When s decreases with temperature reaching minimum and then increase again as shown in Fig. (4.15: c), thus we could argue that overlapping large polaron is the main conduction mechanism up to T≈650K [21]. The crossover from small to large polaron in magnetite as firstly mentioned in the nanometer range could be mainly due to the Fe^{3+} vacancies on the octahedral sites which is highly pronounced above

The high technological applications of functional ferroelectrics encompass about 60% of the total ceramic market [22]. Ferroelectric ceramics have been used in a wide variety of applications and constitute the vast majority of components used in electronics [23].

Mainly; dielectric applications that demand high permittivity in a large frequency range include multilayer capacitors. Moreover, ferroelectric materials in this film could be employed in dynamic random access memories where nonlinear hysteretic dielectric response of the materials is important.

Ferroelectric nanomaterials based systems have demonstrated the potential for very high density data storage. Size confinement of ferroelectric materials may lead to new phenomenon such as of the Curie temperature as a function of crystal size.

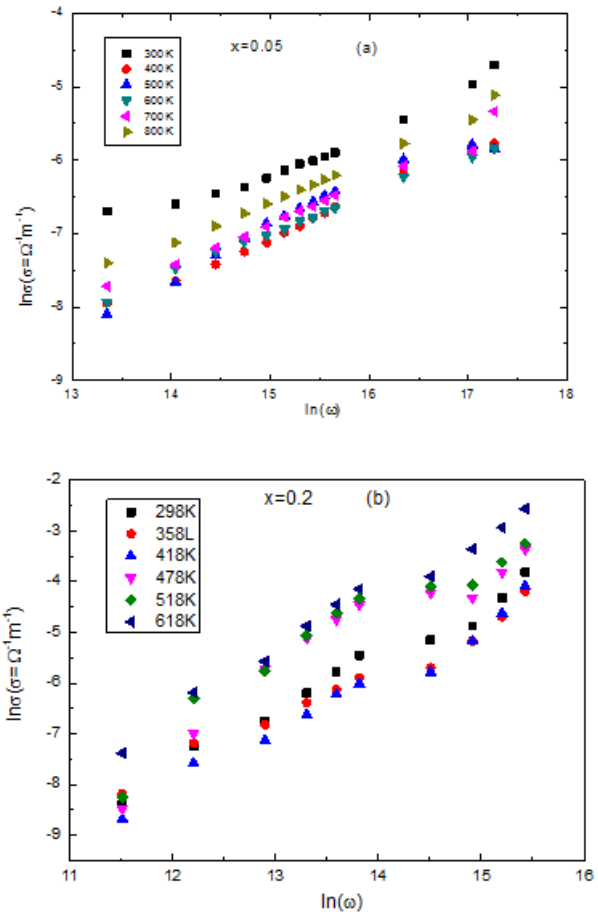

Fig.(3.4) Variation of ln (σ) with Ln (ω) of $La_{0.7}Sr_{0.3}Fe_{1-x}Ni_xO_3$: x=0.05 and 0.2 nanocrystalline samples.

Table (4.2): Dependence of s factor on temperature for the investigated nanomultiferroics.

Ni content(x)	0	0.05	0.1	0.15	0.2
T(K)	S	S	S	S	S
300	0.54	0.43	0.78	0.52	0.54

400	0.30	0.46	0.52	0.44	0.56
500	0.31	0.36	0.48	0.53	0.84
600	0.42	0.39	0.70	0.14	0.70
700	0.40	0.40	0.70	0.18	0.69

3.3. The magnetoelectric Behavior of the multiferroics:

The magnetoelectric nanomaterials consists of ferroelectric and ferromagnetic at which the ME effect is a coupling of two fields in which the electric field induces magnetization and magnetic field induces electric polarization.

The room temperature variation of ME output, ΔE/ΔH as a function of magnetic field H is shown in Fig. (4.) It is well known that the magnetoelectric (ME) coefficient is a measure of change in the resulting electric field in the magnetoelectric orthoferrites due to the applied external magnetic field. The value of ME coefficient depends on the resistivity of the magnetic phase rather than ferroelectric phase. The data obtained that the decreases in the (α) and then increases again up to 0.15 which has the highest value of magnetoelectric coefficient.

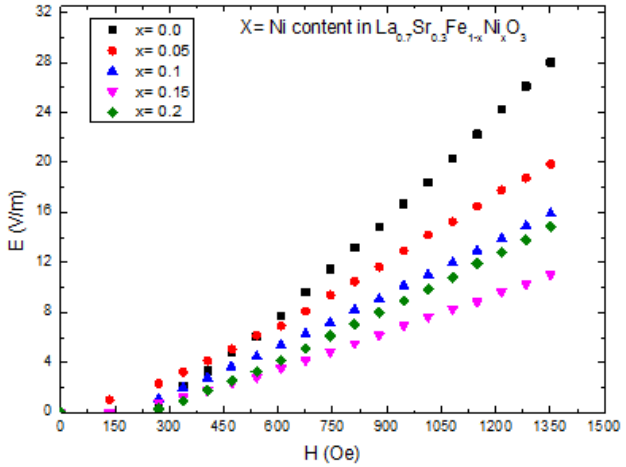

Fig.(3.5) the magnetoelectric coefficient for all nanomultiferroics.

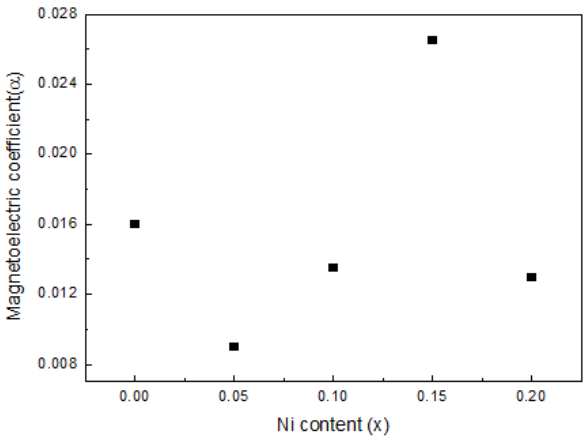

Fig.(3.6) the variation of magnetoelectric coefficient against Ni content for all nanomultiferroics.

3. Seebeck voltage coefficient with average absolute temperature of $La_{0.7}Sr_{0.3}Fe_{1-x}Ni_xO_3$; x= 0.0, 0.05, 0.1, 0.15, and 0.2 nanosamples.

The Seebeck coefficient as function of average absolute temperature is shown in Fig. (4.31:a-e) and the data clarified that negative values, which indicating the presence of electronic conduction up to 475K. The Seebeck coefficient increases with increasing temperature up to 600˚C and then decreases at higher temperatures. The behavior of seebeck coefficient indicates that the number of charge carriers in these materials increase with temperature up to 600˚C and then decrease, for samples x = 0.0, x = 0.05, and x = 0.1 as shown. The other samples at x = 0.15 and 0.2 have the same behavior. This indicates the presence of two predominant conduction mechanisms, electron hopping between Fe^{3+} and Fe^{4+} at the octahedral coordination sites and band conduction. The increase of temperature increases the majority carriers (electrons) because the jump rate of the electrons depends on the temperature, leading to an increase in the thermoelectric power and the number of charge carriers as shown in Fig.(4.13). The first region may be due to mainly extremist band conduction [(24)]. Above 600˚C the decrease of charge carrier concentrations and the thermoelectric power may be due to the substitution of Fe^{3+} ions by Ni^{2+} ions at the B sites which decreases the number of Fe^{3+} ions at the octahedral coordination sites leading to a decrease in the hopping rate of electrons between Fe^{3+} and Fe^{4+}.

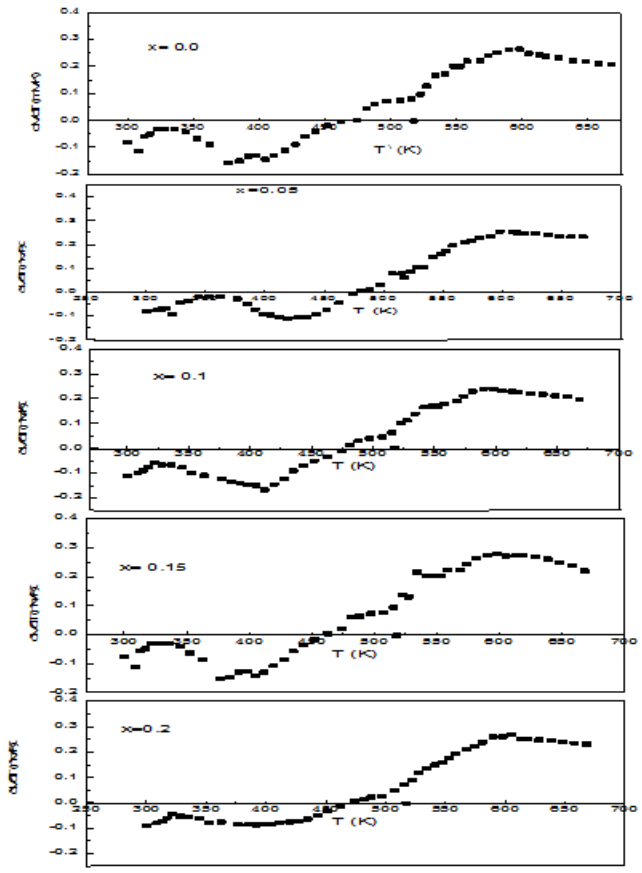

Fig.(4.13:a-e) the variation seebeck voltage coefficient and average absolute temperature for $La_{0.7}Sr_{0.3}Fe_{1-x}Ni_xO_3$; x= 0.0, 0.05, 0.1, 0.15, and 0.2 nanosamples.

4. CONCLUSION:

$La_{0.7}Sr_{0.3}Fe_{1-x}Ni_xO_3$; $0.0 \leq x \leq 0.2$ nanocrystalline samples were prepared successfully using citrate autocombustion technique. Series of samples is limited only up to x = 0.2 composition since the impurity phase starts occurring at this level. Main important results for bulk series are given as underneath:

- The obtained data reveal that ε', and tanδ increase as Ni^{2+} ion increases due to the increase the number of vacancies at the B site as Ni^{2+} content increases.
- The magneto-electric coefficient was measured for all nanomultiferroics samples the higher value of magneto-electric coefficient obtained at x=0.2.
- Above 600˚C the decrease of charge carrier concentrations and the thermoelectric power may be due to the substitution of Fe^{3+} ions by Ni^{2+} ions at the *B* sites which decreases the number of Fe^{3+} ions at the octahedral coordination sites

Reference:

1. K.K. Patanakar, V.L. Mathe, R.P. Mahajan, S.A. Patil, R.M. Reddy, K.V. Sivakumar, Mater. Chem. Phys. 72 (2001) 23.
2. V.L. Mathe, K.K. Patankar, U.V. Jadhav, A.N. Patil, S.A. Patil, Ceram. Int. 27 (2001) 531.
3. S.S. Krotov, A.M. Kadomtseva, Yu.F. Popov, A.K. Zvezdin, G.P. Vorob'ev, D.V. Belov, J. Magn. Magn. Mater. 226 (2001) 963.
4. Yu.F. Popov, A.M. Kadomtseva, G.P. Vorob'ev, V.A. Sonina, M.M. Tehronchi, A.K. Zvezdin, J. Magn. Magn. Mater. 188 (1998) 273.
5. H. Wiegelmann, A.G.M. Jansen, J.P. Rivera, H. Schmid, A.A. Stepanov, I.M. Vitebsky, Physica B 204 (1995) 292.
6. J. B. Goodenough, Theory of the role of covalence in the perovskite-type manganites [La, M(II)]MnO3, Phys. Rev. 100 (1955) 564-573.
7. U. Yu, J. H. Shim, B. H. Kim, B. I. Min, J. Magnetism and Magnetic Materials, 310 (2007) 1660-1662.
8. C. Zener, Phys. Rev. 82 (1951) 403-405.
9. T. Montini, M. Bevilacqua, E. Fonda, M. F. Casula, S. Lee, C. Tavagnacco, R. J. Gorte, P. Fornasiero, Chem. Mater. 21 (2009) 1768-1774.
10. J. B. Torrance, P. Lacorre, A. I. Nazzal, E. J. Ansaldo, C. Niedermayer, Phys. Rev. B, 45 (1992) 8209-8212.
11. H. Falcon, A. E. Goeta, G. Punte, R. E. Carbonio, J. Solid State Chemistry 133 (1997) 379-385.
12. M. Medarde, J. Mesot, S. Rosenkranz, P. Lacorre, W. Marshall, S. Klotz, J. S. Loveday, G. Hamel, S. Hull, P. Radaelli, Physica B 234-236 (1997) 15-17.
13. M.A. Ahmed, S.I. El-Dek, A. Abd Elazim, superlattices and microstructures, 74(2014) 34-51.
14. G.V. Subba Rao, C.N.R. Rao, Appl. Spectrosc. 24 (1970) 436.
15. [Amin, N., Arajs, S., and Matijevic, E., Phys.Status Solidi A 104, K65(1987).
16. A. K.J. Jonscher, Dielectric relaxation in solid, Chelska Dielectric Press, Limited, London (1987).
17. S. R. Elliott, Advances in Phys-ics, 36, 2 (1987) 135.
18. S. Erat, A. Braun, A. Ovalle, C. Piamonteze, Z. Liu, T. Graule, L. J. Gauckler, Correlation of O (1s) and Fe (2p) near edge x-ray absorption fine structure spectra and electrical conductivity of La1−xSrxFe0.75Ni0.25O3−δ, Appl. Phys. Lett. 95 (2009) 174108 1-3.
19. K. S. Ryu, S. J. Lee, C. H. Yo, Studies of nonstoichiometric and physical properties of the perovskite SrxHo1-xFeO3-y system, Bull. Korean Chem. Soc. 15 (1994), 256-260.
20. A. K.J. Jonscher, Dielectric relaxation in solid, Chelska Dielectric Press, Limited, London (1987).
21. S.R. Elliott, Adv. Phys. 36 (1987) 135.
22. Y. Y. Guo, H. M. Liu, D. P. Yu, and J.-M. Liu, Phys. Rev. B 85, 104108 (2012) (6Pages).
23. Minoru Soda, Masato Matsuura, Yusuke Wakabayashi, and Kazuma Hirota, J. Phys. Soc. Jpn. 80 (2011) 043705 (4Pages).